Arteriosclerosis, Thrombosis, and Vascular Biology

TRANSLATIONAL SCIENCES

Platelet Dysfunction and Thrombosis in JAK2^{V617F}-Mutated Primary Myelofibrotic Mice

Shinobu Matsuura,* Cristal R. Thompson,* Mostafa Elmokhtra Belghasem, Roelof H. Bekendam, Andrew Piasecki, Orly Leiva, Anjana Ray, Joseph Italiano, Moua Yang, Glenn Merill-Skoloff, Vipul C. Chitalia, Robert Flaumenhaft, Katya Ravid

OBJECTIVE: The risk of thrombosis in myeloproliferative neoplasms, such as primary myelofibrosis varies depending on the type of key driving mutation (JAK2 [janus kinase 2], CALR [calreticulin], and MPL [myeloproliferative leukemia protein or thrombopoietin receptor]) and the accompanying mutations in other genes. In the current study, we sought to examine the propensity for thrombosis, as well as platelet activation properties in a mouse model of primary myelofibrosis induced by JAK2^{V617F} (janus kinase 2 with valine to phenylalanine substitution on codon 617) mutation.

APPROACH AND RESULTS: Vav1-hJAK2^{V617F} transgenic mice show hallmarks of primary myelofibrosis, including significant megakaryocytosis and bone marrow fibrosis, with a moderate increase in red blood cells and platelet number. This mouse model was used to study responses to 2 models of vascular injury and to investigate platelet properties. Platelets derived from the mutated mice have reduced aggregation in response to collagen, reduced thrombus formation and thrombus size, as demonstrated using laser-induced or $FeCl_3$-induced vascular injury models, and increased bleeding time. Strikingly, the mutated platelets had a significantly reduced number of dense granules, which could explain impaired ADP secretion upon platelet activation, and a diminished second wave of activation.

CONCLUSIONS: Together, our study highlights for the first time the influence of a hyperactive JAK2 on platelet activation-induced ADP secretion and dense granule homeostasis, with consequent effects on platelet activation properties.

GRAPHIC ABSTRACT: A graphic abstract is available for this article.

Key Words: bone marrow ■ calreticulin ■ megakaryocytes ■ platelets ■ primary myelofibrosis ■ thrombosis

Philadelphia chromosome negative myeloproliferative neoplasms (MPN) include polycythemia vera (PV), essential thrombocytosis (ET), and primary myelofibrosis (PMF). The latter 3 are typically classified according to somatic mutations mainly in 3 genes (*JAK2* [janus kinase 2], *CALR* [calreticulin], and *MPL* [myeloproliferative leukemia protein]) combined with abnormalities in the myeloid lineage. PMF consists of augmented proliferation of megakaryocytes, fibrosis in the bone marrow, and presence of a clonal marker.[1,2] The classification by the World Health Organization makes a distinction between pre-PMF and overt PMF, the main difference being the presence of fibrosis in overt PMF.[3]

Several mouse models of Philadelphia chromosome-negative MPN have been developed.[4] Most recent focus has been on incorporating the JAK2^{V617F} (janus kinase 2 with valine to phenylalanine substitution on codon 617) mutation in the myeloid lineages through knock-in (KI). Differences in expression of the JAK2^{V617F} mutation appear to correlate with the phenotypic manifestations.[4] Differentiating between PV, ET, and PMF is pivotal as the clinical presentation, the prognosis, and propensity for thrombosis are heterogeneous in these patient populations.[5] Expression of JAK2^{V617F} in KI murine models at similar levels or higher than wild-type (WT) JAK2 is associated with a PV-like phenotype, whereas

Correspondence to: Katya Ravid, Boston University School of Medicine, 700 Albany St, W-6, Boston, MA 02118. Email kravid@bu.edu
*These authors contributed equally to this article.
The Data Supplement is available with this article at https://www.ahajournals.org/doi/suppl/10.1161/ATVBAHA.120.314760.
For Sources of Funding and Disclosures, see page e271.

Arterioscler Thromb Vasc Biol is available at www.ahajournals.org/journal/atvb

Nonstandard Abbreviations and Acronyms

AUC	area under the curve
CALR	calreticulin
ET	essential thrombocythemia
GPVI	platelet glycoprotein VI
JAK2^{V617F}	janus kinase 2 with valine to phenylalanine substitution on codon 617
KI	knock-in
MPL	myeloproliferative leukemia protein or thrombopoietin receptor
MPN	myeloproliferative neoplasms
Plek2	pleckstrin-2
PMF	primary myelofibrosis
PV	polycythemia vera
WT	wild-type

Highlights

- The Vav1-hJAK2^{V617F} transgenic mice show prolonged bleeding time and reduced thrombus formation and thrombus size using 2 in vivo models of vascular injury.
- Washed platelets from Vav1-hJAK2^{V617F} mice have reduced aggregation in response to collagen, and reduced expression of α2 integrin subunit and GPVI (platelet glycoprotein VI).
- ADP secretion is reduced in activated mouse JAK2^{V617F} (janus kinase 2 with valine to phenylalanine substitution on codon 617) platelets.
- Dense granule number is reduced in JAK2^{V617F} platelets.

expression levels of JAK2^{V617F} lower than WT JAK2 results in increased platelet levels consistent with an ET-like phenotype.[6,7]

All Philadelphia chromosome-negative MPN have an increased thrombogenic tendency.[8] Overall, arterial or venous thrombosis in patients with PMF has been shown to be ≈20%.[9] All MPN, including PMF, have an increased tendency to develop Budd-Chiari syndrome, involving vein occlusion.[10] Unlike PV and ET, hemorrhagic events are more common in PMF (≈10% versus 3%).[11] Mimicking thrombogenic phenotypes in mouse models has uncovered heterogeneity which is also observed in patients with MPN. Several JAK2^{V617F} models exist and exhibit different characteristics on the spectrum of MPN. For example, one human JAK2^{V617F} KI model exhibited a more ET-like phenotype with observed megakaryocyte and platelet hyperactivation.[7] In this instance, the mice were heterozygous for the JAK2^{V617F} mutation. In later studies, the same group showed that homozygous JAK2^{V617F} mutation resulted in a more profound PV-like phenotype with marked erythrocytosis and increased platelet turnover.[12] On the contrary, a JAK2^{V617F} KI mouse model showed hyporesponsive platelets, a mild GPVI (platelet glycoprotein VI) deficiency in vitro and rapid occlusive, but unstable clots in vivo.[6] These examples illustrate that the heterogenicity of hemostatic disorders observed in mouse models likely depends on the level and site of JAK2^{V617F} mutation. Indeed, new evidence indicates that endothelial cells[13] and neutrophils are contributing to the increased thrombosis in MPN through neutrophil extracellular traps.[14] Endothelial cells contribute in the ET phenotype to an acquired von Willebrand deficiency, resulting in increased bleeding tendency.[13] In the current study, we sought to examine propensity for thrombosis and platelet activation properties in a transgenic mouse model in which human JAK2^{V617F} is expressed in megakaryocytes. This mouse line shows hallmarks of PMF including significant megakaryocytosis and bone marrow fibrosis, with moderate increase in red blood cells and platelet number.[15]

MATERIALS AND METHODS

The authors declare that all supporting data are available within the article (and it is in the Data Supplement).

JAK2^{V617F} Transgenic Mice

Vav1-hJAK2^{V617F} (JAK2^{V617F}) mice were gift from Dr Zhizhuang Joe Zhao (University of Oklahoma). The mouse line A, harboring 13 copies of the transgene, has the hallmarks of PMF, including expansion of the megakaryocyte lineage, a fibrotic bone marrow and splenomegaly (Figure IA in the Data Supplement).[15,16] Expansion of the mouse colonies was performed at Boston University School of Medicine, and all studies involving mice were approved by the Boston University Institutional Animal Care and Use Committee. Animal housing conditions and treatment protocols were approved by the Institutional Animal Care and Use Committee of Boston University School of Medicine.

Peripheral Blood Analysis

Peripheral blood collection was performed via retro-orbital plexus bleeding using a heparinized capillary tube in animals under isoflurane anesthesia. Blood parameters were measured in blood collected in EDTA tubes (Sarstedt, Germany) using a Hemavet HV950FS hematology counter (Drew Scientific, Waterbury, CT).

Vascular Injury Models

The carotid artery injury model of vascular thrombosis was performed as previously described.[17] Mice were anesthetized by 5% isoflurane gas and placed on a temperature-regulated pad to maintain body temperature at 37°C. The right carotid artery was exposed and basal blood flow recorded using a 0.5PSB S-Series flowprobe connected to a TS420 perivascular transit-time flow meter (Transonic, Ithaca, NY). The probe

was removed, and a piece of Whatman filter paper (1×3 mm) soaked in 7.5% ferric chloride ($FeCl_3$; Sigma-Aldrich, St. Louis, MO) was placed in the artery for 1 minute. The probe was then placed on the carotid artery downstream of the injury site, and the flow of blood was measured for a maximum of 25 minutes starting from the placement of the filter. The mean, maximum, and minimum carotid flow was recorded using Powerlab Chart5 version 5.2 software in 1-second intervals. Time to occlusion was determined as the first measurement ≤0.299 mL/min.

For laser-injury thrombosis experiments, animal care and experimental procedures were performed in accordance with and under the approval of the Beth Israel Deaconess Medical Center Institutional Animal Care and Use Committee. Mice were anesthetized with intraperitoneal injection of a ketamine (125 mg/kg) and xylazine (12.5 mg/kg) mixture in sterile saline. Anesthesia was maintained with pentobarbital (5 mg/kg) through a jugular vein cannula. The intravital fluorescence microscopy system has previously been described.[18] Modifications of the imaging system that were used for these studies include an Orca-Flash 4.0 sCMOS camera (Hamamatsu-Hamamatsu City, Japan) to capture digital video images, a LED-based SpectraX light engine (Lumencor-Beaverton, OR) using 6 solid state light sources, and a LED-based white light source (Prior Scientific-Rockland, MA). Cremaster arterioles were injured using a MicroPoint Laser system (Photonics Instruments). We use a cremaster preparation since this surgical window provides access to a microvasculature that is mostly free of connective tissue and can be accessed with minimal trauma to the vessel. Other preparations are associated with more connective tissue, which can interfere with the path of the laser, and trauma, which can activate leukocyte rolling and affect thrombus formation. Since only male mice have a cremaster muscle, only male mice are used for these studies. Ablation injuries were observable by white-light trans illumination of the cremaster muscle, presenting as a distortion of the vessel wall in the region adjacent to the injury site. This distortion was quantified by measuring the length of the disrupted region in micrometers. All ablation injury measurements were obtained from the frame immediately following injury for consistency. Data from WT mice (35 thrombi, 4 mice) and Vav1-hJAK2^{V617F} mice (31 thrombin, 3 mice) were used to determine the median value of the integrated fluorescence intensity to account for the variability of thrombus formation at any given set of experimental conditions. Data were analyzed using Slidebook 6.0 (Intelligent Imaging Innovations).

Tail Bleeding Time

Mice induced and maintained by isoflurane anesthesia were placed on a heat pad, and 3 mm of tail tip was cut with a scalpel and immersed immediately in saline (0.9% NaCl) at 37°C in 50 mL conical tube. Time to cessation of blood stream was measured and recorded. Absence of bleeding for 1 minute was considered complete cessation. Bleeding is observed for a total of 20 minutes from the cutting of the tail, including partial cessations that resume within 1 minute.[19]

Isolation of Washed Platelets and Platelet Aggregation Assay

Blood was collected via retro-orbital plexus in 10% final volume of acid-citrate-dextrose anti-coagulant solution (85 mmol/L trisodium citrate dihydrate, 66.6 mmol/L citric acid monohydrate, 111 mmol/L dextrose, 450 mOsm/L, pH 4.5) and diluted with modified Tyrode buffer (137 mmol/L NaCl, 11.9 mmol/L $NaHCO_3$, 0.4 mmol/L Na_2HPO_4, 2.7 mmol/L KCl, 1.1 mmol/L $MgCl_2$, 5.6 mmol/L glucose, pH 7.3) and centrifuged at 100*g* for 30 minutes. Platelet-rich plasma and buffy coat were transferred to a new tube and centrifuged at 100*g* for 20 minutes. Prostacyclin (Sigma Aldrich, St. Louis, MO) was added at 1 µg/mL, and apyrase (Sigma Aldrich, St. Louis, MO) was added at 2 U/mL. Platelets were then pelleted at 900*g* for 7 minutes and resuspended in modified Tyrode buffer for quantitation on the Hemavet HV950FS hematology counter and diluted to the appropriate concentration. Platelet aggregation was monitored in a PAP-4 aggregometer equipped with a micro-volume adaptor (Bio/Data Corporation, Horsham, PA) at 37°C for 6 minutes, at 1200 rpm stirring speed, as previously described.[17] Aggregation was performed with 180 µL of washed platelets at 1.0×10^8 platelets/mL, added with 20 µL of murine thrombin (Enzyme Research Laboratories, South Bend, IN), acid-soluble calf skin type I collagen (Bio/Data Corp, Horsham), and ADP (Bio/Data) with doses indicated in figures.

Flow Cytometry

Flow cytometry analysis of washed platelets was completed as previously described.[17] For analysis of GPVI, α2 integrin subunit, and β1 integrin subunit expression, washed platelets

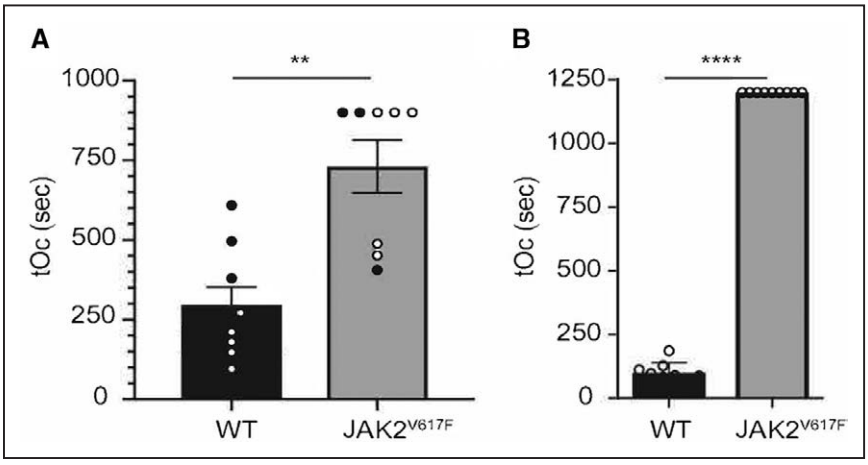

Figure 1. JAK2V617F (janus kinase 2 with valine to phenylalanine substitution on codon 617) mice show prolonged time to occlusion in a FeCl3 model of vascular injury, as well as prolonged bleeding.
A, Carotid artery injury was performed on wild-type (WT; n=8) and JAK2^{V617F} (n=9) male mice. Time to occlusion (tOc) for each mouse in shown. Black circles represent mice 12 wk old, open circles represent mice age 30 wk old. Data are averages±SD. **B**, Tail bleeding assay of WT (n=9) and JAK2^{V617F} (n=9) male mice 14–20 wk old. $^{**}P<0.01$, $^{****}P<0.0001$, unpaired 2-tailed *t* test.

Table 1. Analysis of Blood Fibrinogen and Prothrombin Time in WT and JAK2^{V617F} Plasma

	Prothrombin Time, sec*	Fibrinogen, mg/dL*
WT†	12.2±0.7 (n=5)	222.6±77.0 (n=5)
JAK2^{V617F}†	11.7±0.9 (n=4)	281.5±67.7 (n=4)
P value‡	NS	NS

JAK2V617F indicates janus kinase 2 with valine to phenylalanine substitution on codon 617; NS, nonsignificant; and WT, wild-type.
*Data are mean values±SD.
†4–5 WT and JAK2^{V617F} female mice, ≈30 wk old.
‡Unpaired 2-tailed *t* test.

were incubated for 30 minutes in modified Tyrode buffer with the following antibodies: PE conjugated anti-mouse CD41a (eBioscience, catalog No. 12-0411-83); FITC conjugated rat anti-mouse GPVI (Emfret Analytics, catalog No. M011-1); anti-mouse CD49b FITC (α2 subunit; eBioscience, catalog No. 11-0491-82); anti-rat CD29 Alexa Fluor 647 (β1 subunit; BD Pharmingen, catalog No. 562153). For analysis of P-selectin expression in agonist-stimulated platelets, platelets were resuspended at 1×10^8 platelets/mL, aliquoted into tubes and stained with FITC Rat anti-mouse CD62p (P-selectin; BD Pharmingen, catalog No. 553744) and APC Rat anti-mouse CD41a (eBioscience, catalog No. 17-0411-82). Acid-soluble calf skin type I collagen (Bio/Data Corp, Horsham) were added with doses indicated in figures. Samples were analyzed after 15 minutes of incubation at room temperature. Cells were analyzed on the LSRII flow cytometer using FACS Diva software (BD Biosciences) and FlowJo (Becton, Dickinson and Company).

Platelet Granule ADP and ATP Measurement

Platelets were isolated from whole blood as described above. Fifty microliters of 10^8 platelets/mL per reaction were prepared. Agonist was added at the indicated doses and incubated with platelets for the indicated time, followed by centrifugation at 900*g* for 1 minutes. The supernatant was used to measure ADP and ATP secretion using the Abcam ADP/ATP Ratio Assay Kit (Abcam ab65313, Cambridge, MA) per manufacturer's instructions. Technical duplicates for each biological replicate were performed. Phorbol-myristate-acetate (Sigma) was dissolved as per manufacture instructions.

Electron Microscopy

Platelets were isolated from whole blood as described above. Platelets from the same mouse line were pooled and centrifuged at 900*g* for 15 minutes. A volume of ≈50 to 100 µL of platelet pellets was supplemented with about 200 µL of modified Tyrode buffer (137 mmol/L NaCl, 11.9 mmol/L $NaHCO_3$, 0.4 mmol/L Na_2HPO_4, 2.7 mmol/L KCl, 1.1 mmol/L $MgCl_2$, 5.6 mmol/L glucose, pH7.3). Then, a volume of 1.3 mL of formaldehyde/glutaraldehyde, 2.5% each in 0.1 mol/L sodium cacodylate buffer (fixative) pH 7.4 at 37°C was added to the solution of platelets. Pellets were allowed to incubate in fixative for 5 minutes and then pelleted and resuspended in fixative again and allowed to fix overnight. Pellets were stored in cacodylate buffer (Electron Microscopy Sciences 11652, Hatfield, PA) until ready for electron microscopy analysis. For thin-section electron microscopy, platelets were fixed with 1.25% paraformaldehyde, 0.03% picric acid, 2.5% glutaraldehyde in 0.1 mol/L cacodylate buffer (pH 7.4) for 1 hour, postfixed with 1% osmium tetroxide, dehydrated through a series of alcohols, infiltrated with propylene oxide, and embedded in epoxy resin. Ultrathin sections were stained and examined with a Tecnai G2 Spirit BioTwin electron microscope (Hillsboro, OR) at an accelerating voltage of 80 kV. Images were recorded with an Advanced Microscopy Techniques 2-K charged coupled device camera, using Advanced Microscopy Techniques digital acquisition and analysis software (Advanced Microscopy Techniques, Danvers, MA).

Measurement of Blood Fibrinogen and Prothrombin Time

Plasma was collected per IDEXX Laboratories (Westbrook, Maine) instructions. Briefly, whole blood was collected in 3.2% citrate at a 1:9 ratio of citrate: whole blood and centrifuged at 1500 rpm, 15 minutes. Plasma was collected, frozen, and shipped to IDEXX for analysis.

Statistical Analysis

Statistical analysis was performed using GraphPad Prism. Student *t* test and Mann-Whitney *U* test with an α of at least 0.05 were considered significant. Normality and variance were not tested. As described in a previous publication,[20] the platelet accumulation and fibrin formation data do not demonstrate a normal distribution. For this reason, the nonparametric analysis Mann-Whitney test was used for these data. In the Mann-Whitney nonparametric *U* test, the values are ranked from low to high and the *P* values were calculated based on the ranks of the 2 groups. Area under the curves (AUC) were extrapolated from Igor Pro using the trapezoid method based on the equation:

$$(\Delta X \times \frac{(Y_1 + Y_2)}{2})$$

Please see the Major Resources Table in the Data Supplement.

Table 2. Peripheral Blood Complete Blood Count

	WBC, 10^3/µL*	RBC, M/µL*	Hb, g/dL*	HCT, %*	PLT, K/µL*
WT†	8.1±2.6	6.2±0.3	7.5±0.83	27.8±2.2	709.3±77.1
JAK2^{V617F}†	17.0±6.9	6.9±0.74	6.1±1.0	25.4±3.4	1010.7±558.6
P value‡	NS	NS	NS	NS	0.021

Hb indicates hemoglobin; HCT, hematocrit; JAK2V617F, janus kinase 2 with valine to phenylalanine substitution on codon 617; NS, nonsignificant; PLT, platelet count; RBC, red blood cell count; WBC, white blood cell count; and WT, wild-type.
*Data are mean values±SD, 4 biological replicates.
†Male mice, ≈30 wk old.
‡Unpaired 2-tailed *t* test.

RESULTS

JAK2^{V617F} Mice Show Decreased Time to Occlusion in Vascular Injury Models of Thrombosis

The Vav1-hJAK2^{V617F} mouse model of PMF was subjected to $FeCl_3$-induced vascular injury. Both young and older JAK2^{V617F} mice showed prolonged time to occlusion (Figure 1A) and prolonged tail bleeding time (Figure 1B), compared with matching controls. Since older JAK2^{V617F} mice have significant bone marrow fibrosis, we conclude that myelofibrosis per se is not a significant determinant of the thrombotic response in these mice, compared with younger JAK2^{V617F} mice. Analysis of plasma isolated from the experimental groups indicated that fibrinogen level as well as prothrombin time (indicative of plasma coagulation properties) were similar in JAK2^{V617F} and matching

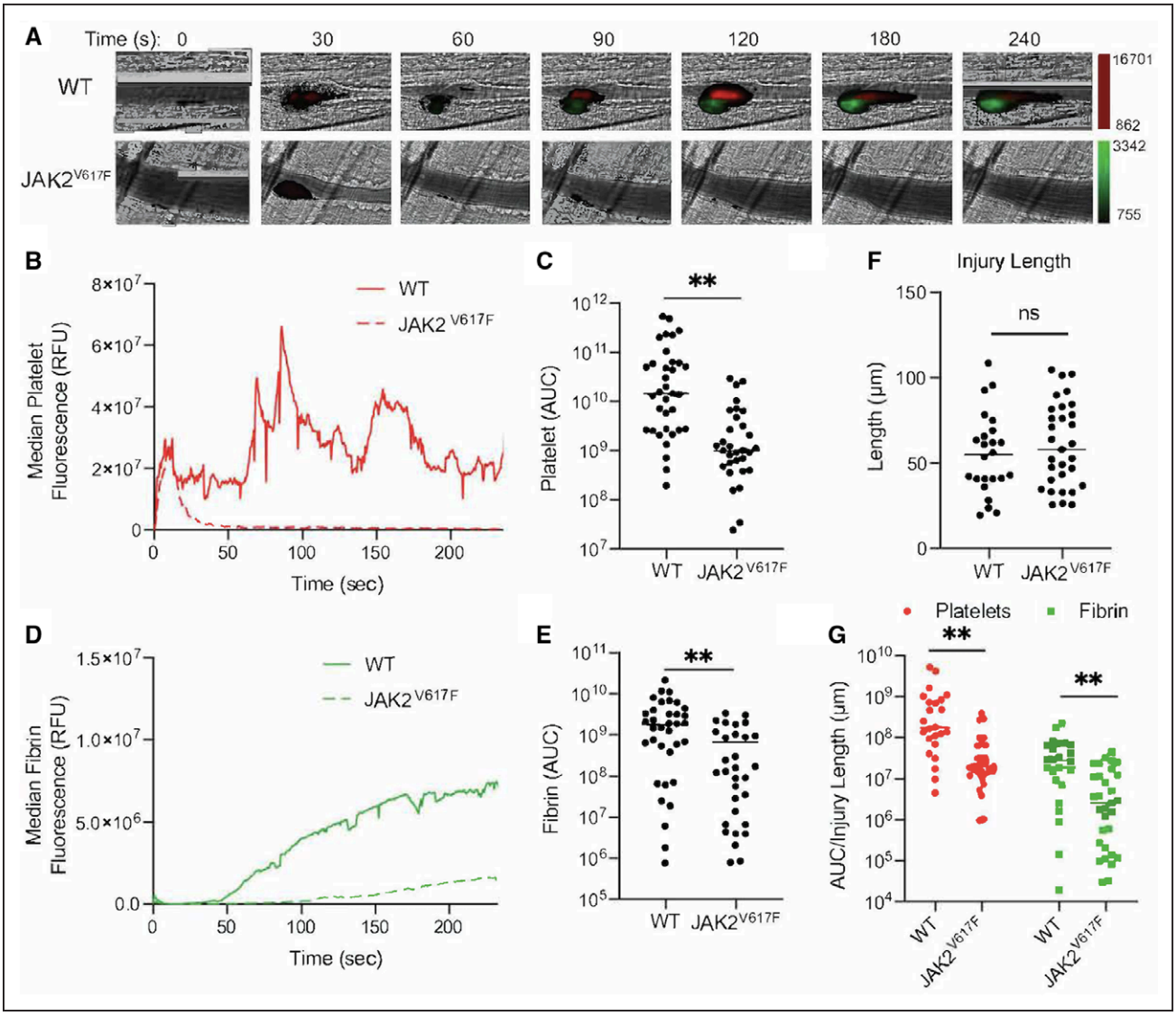

Figure 2. JAK2V617F (janus kinase 2 with valine to phenylalanine substitution on codon 617) mice demonstrate decreased platelet accumulation and fibrin formation.

A, Approximately 28.4-wk-old males (n=5 each) wild-type (WT) and JAK2^{V617F} mice were injected with Dylight 647-labeled anti-platelet antibody (CD42b) and Dylight 488-labeled anti-fibrin antibody (59D8). Representative images obtained at the indicated times following laser-induced injury are shown. Fluorescence intensity in each channel was normalized to background fluorescence obtained from images before laser-induced injury. **B**, Median integrated platelet intensities following laser injury were calculated and plotted at 0.5 sec intervals for all thrombi in WT (n=35 thrombi) and Vav1-hJAK2^{V617F} mice (n=31 thrombi). **C**, Platelet AUCs were calculated and plotted for each thrombus formed in WT and Vav1-hJAK2^{V617F} mice. Median values are indicated. **D**, Median integrated fibrin intensities following laser injury were calculated and plotted at 0.5 sec intervals for all thrombi in vehicle and Vav1-hJAK2^{V617F} mice. **E**, Fibrin AUCs were calculated and plotted for each thrombus formed in WT and Vav1-hJAK2^{V617F} mice. Median values are indicated. **F**, Ablation injury lengths were measured in WT and Vav1-hJAK2^{V617F} mice as a marker of injury severity. Median values were plotted. **G**, Platelet accumulation and fibrin formation data were normalized for injury severity by dividing the area under the curve (AUC) value for each thrombus by its corresponding ablation injury length. ns indicates not significant. **$P<0.01$, Mann Whitney U test.

WT control mice (Table 1). Of note, platelet counts were slightly higher in JAK2^{V617F} mice compared with controls, as typical of PMF (blood cell count is shown in Table 2).

We used intravital microscopy to monitor platelet accumulation and fibrin formation in real-time following laser-induced injury of cremaster arterioles. Platelets and fibrin were visualized using Dylight 647-labeled anti-platelet antibody (CD42b) and Dylight 488-labeled anti-fibrin antibody (59D8). Both platelet accumulation and fibrin formation were impaired in Vav1-hJAK2^{V617F} mice compared with controls (Figure 2A through 2E). Vav1-hJAK2^{V617F} mice showed decreased platelet accumulation over time compared with control mice (Figure 2B). Total platelet accumulation as determined by AUC analysis indicated a median value of 9.92×10^{8} in Vav1-hJAK2^{V617F} mice whereas control mice showed a median AUC value of 1.44×10^{10} ($P<0.01$; Figure 2C), indicating a >14-fold reduction in platelet accumulation. The kinetics of fibrin formation were also decreased in Vav1-hJAK2^{V617F} mice (Figure 2D), with median fibrin AUC measurements indicating 1.34×10^{8} in Vav1-hJAK2^{V617F} mice and 1.74×10^{9} in control mice ($P<0.01$; Figure 2E). Differences in thrombus formation can occur from differences in injury severity. To determine whether

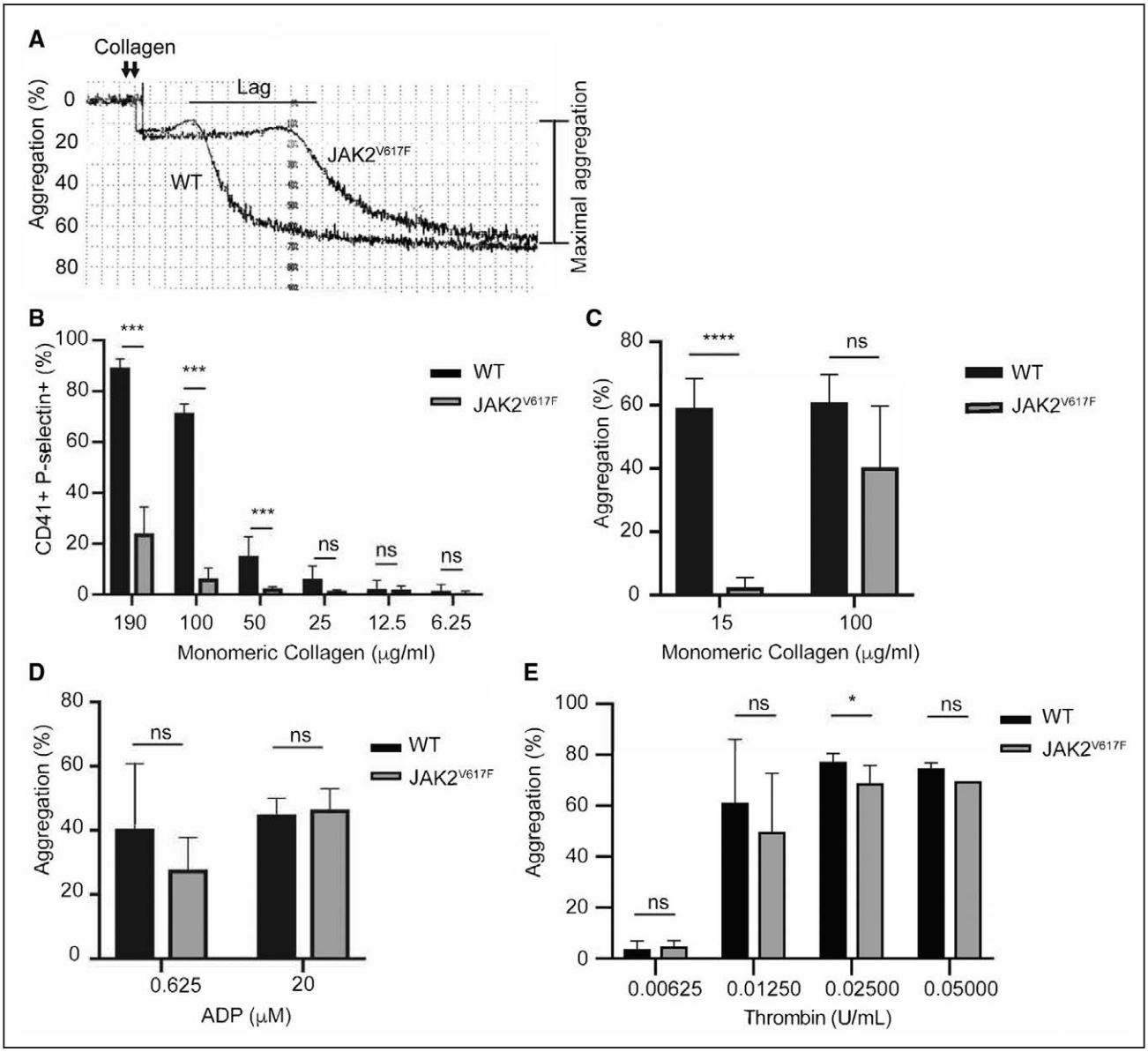

Figure 3. JAK2V617F (janus kinase 2 with valine to phenylalanine substitution on codon 617) platelets exhibit decreased platelet aggregation response to collagen.

A, Representative aggregation trace of platelets derived from 15 wk old males JAK2^{V617F} and wild-type (WT) mice, activated by 10 μg/mL monomeric collagen. The tracing is representative of at least 3 biological replicates. **B**, Flow cytometry of 10 wk old females WT (n=3) and JAK2^{V617F} (n=4) washed platelets labeled with CD41 (platelet marker) and *P*-selectin after activation with monomeric collagen at the indicated concentrations. Platelet aggregation as measured in response to indicated concentrations of collagen (**C**) ADP (**D**) and thrombin (**E**), using 5 to 6 15 wk old male mice in each case. Data are averages±SD. ns indicates not significant. **P*<0.05, ****P*<0.001, *****P*<0.0001.

reduced thrombus formation in the Vav1-hJAK2^{V617F} mice resulted from decreased injury sizes, we measured ablation injury length in Vav1-hJAK2^{V617F} and control mice. No significant differences in injury size were detected (Figure 2F). Furthermore, when platelet accumulation and fibrin formation for individual thrombi were normalized on the basis of injury size, differences in the median normalized platelet accumulation (2.0×10^7 AUC/injury length in Vav1-hJAK2^{V617F} mice versus 2.4×10^8 AUC/injury length in controls) and fibrin formation (2.80×10^6 AUC/injury length in Vav1-hJAK2^{V617F} mice versus 2.99×10^7 AUC/injury length in controls) persisted ($P<0.01$: Figure 2G). These data indicate that platelet accumulation and fibrin formation are defective in Vav1-hJAK2^{V617F} mice despite demonstrating similar injury sizes following laser ablation of arterioles.

Platelet Aggregation Response to Collagen Is Compromised in JAK2^{V617F} Mice

Platelets derived from age- and sex-matched control and JAK2^{V617F} mice were tested for their response to different agonists. Of the ones tested, collagen seemed to induce less platelet aggregation in the mutated mice, compared with controls (Figure 3A through 3C). Activation by ADP was comparable in the experimental groups at higher doses, but at lower doses a tendency for impaired aggregation was observed in JAK2^{V617F} platelets (Figure 3D), and one concentration of thrombin had a slightly reduced effect on JAK2^{V617F} platelets compared with controls (Figure 3E). Myelofibrosis did not seem to affect platelet response to agonists as the defect was consistently observed between young (nonmyelofibrotic) and old (myelofibrotic) mice (Figure IB and IC in the Data Supplement). The major receptors for collagen are $\alpha2\beta1$ and GPVI. Flow cytometry analysis of the level of these receptors on platelet surface indicated a reduction in the level of $\alpha2$ and GPVI, but not of $\beta1$ in JAK2^{V617F} mice, compared with matching controls (Figure 4). This JAK2 mutation-induced changes in the above integrins could explain a compromised platelet aggregation response to collagen in the mutated mice.

Platelet ADP and ATP Secretion

Tracing aggregation kinetics revealed that while WT platelets have a sharp aggregation response, typically mediated by a second wave of activation induced by

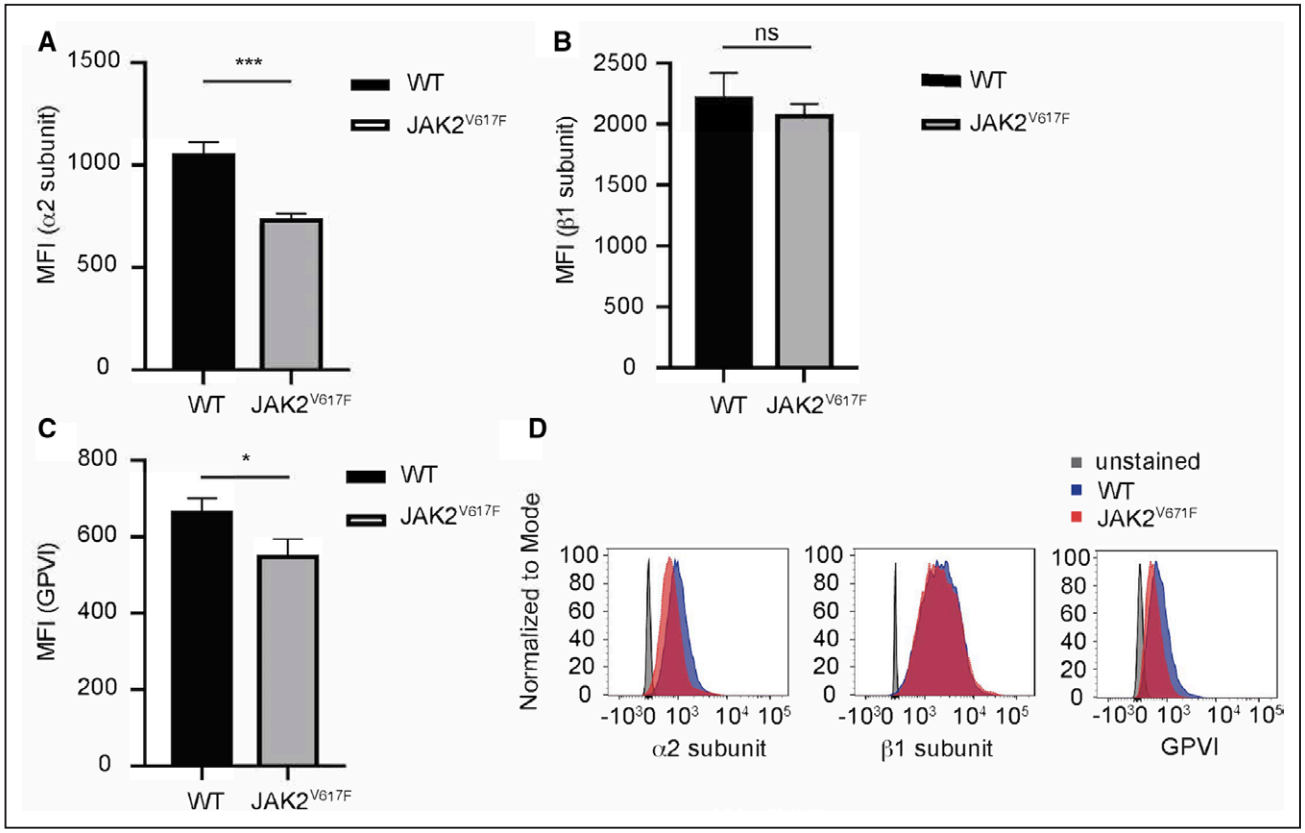

Figure 4. JAK2V617F (janus kinase 2 with valine to phenylalanine substitution on codon 617) platelets show decreased cell surface levels of α2 integrin subunit and GPVI.
Platelets derived from JAK2^{V617F} and wild-type (WT) mice (as in Figure 3) were subjected to flow cytometry analysis to measure cell surface $\alpha2$ integrin subunit (**A**), $\beta1$ integrin subunit (**B**), and GPVI (platelet glycoprotein VI; **C**), using antibodies as described under Methods in the Data Supplement. A representative flow cytometry tracing is shown in **D**. Data are averages±SD. Fifteen week old male WT and JAK2^{V617F} mice (n=3 each). ns indicates not significant. *$P<0.05$; ***$P<0.001$.

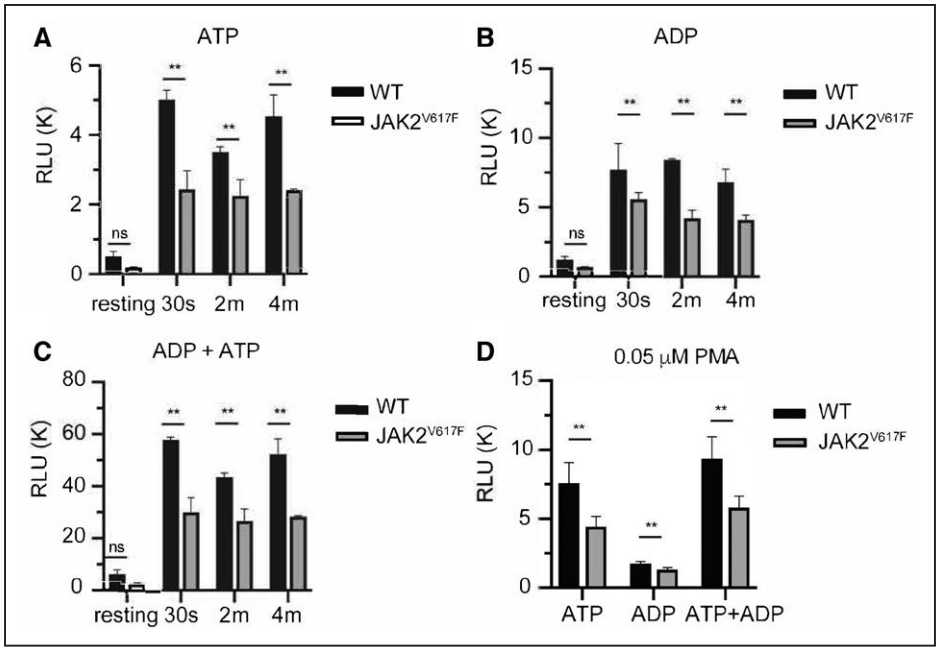

Figure 5. JAK2V617F (janus kinase 2 with valine to phenylalanine substitution on codon 617) platelets show decreased secretion of ADP and ATP in response to collagen activation.
Extracellular (**A**) ADP, (**B**) ATP, and (**C**) ADP+ATP were measured in response to 10 μg/mL monomeric collagen (see Methods in the Data Supplement). For this set of analysis, 3 separate experiments were performed with a total of 7 male mice; 4 mice 26–30 wk of age, and 3 mice 15 wk of age. Data are averages±SD. Results were collectively averaged as the trend was similar in the young and older mice. **D**, Platelets were activated by a concentration of phorbol-myristate-acetate (PMA; 0.05 μmol/L) found following preliminary exploration to activate platelets and to induce ATP and ADP release. Values of secreted nucleotides are shown. Data are averages±SD of n=4 male mice, 14 wk of age. ns indicates not significant; RLU, relative light units; and WT, wild-type. $^{**}P<0.01$.

intracellularly released ATP/ADP, the response was shallower in platelets of the JAK2^{V617F} mice, before reaching a plateau (Figure 3A). This, plus the appearance of smaller thrombi in JAK2^{V617F} mice subjected to vascular injury (Figure 2B) led us to suspect that ATP/ADP secretion is compromised in JAK2^{V617F} platelets. To examine this possibility, the release of ATP and ADP was measured following collagen-induced platelet activation. Interestingly, ATP and ADP release by JAK2^{V617F} platelets was significantly reduced compared with controls (Figure 5A through 5C). Platelet activation by phorbol-myristate-acetate, a calcium ionophore known to induce platelet aggregation and secretion,[18] also resulted in diminished extracellular ADP and ATP in JAK2^{V617F} samples compared with controls (Figure 5D). Considering that ADP/ATP is stored in and released from platelet dense granules, we sought to examine the platelet ultrastructure in the experimental samples. Electron microscopy analysis showed a significantly reduced number of dense granules in platelets of JAK2^{V617F} mice compared with controls, suggesting that JAK2 hyperactivating mutation affects the development and assembly of these granules (Figure 6).

DISCUSSION

A recent population-based study[21] of 9429 patients with different forms of MPNs and 35 820 matched control participants found that the calculated hazard ratio for venous thrombosis was about 3-fold greater than for arterial thrombosis across all age groups and among all MPN subtypes, compared with controls, although the degree of venous thromboembolism seems to vary between ET, PV, and PMF. MPN patients with high JAK2^{V617F} allele burden are prone to developing complications associated with hemorrhages and thrombosis.[22,23] Development of pathological thrombosis is controlled by an array of factors, such as platelet activation, changes in hyperviscosity and shear stress affected by an increase in red blood cell level, changes inflammatory cytokines and white blood cells activation, the integrity of the endothelium, and coagulation factors. A combination of some or all of these conditions in patients with PMF will be affected by the type of MPN and could influence which patients develop venous and arterial thrombosis or hemorrhages.

The complexity of the human MPN condition is amplified by secondary accessory mutations that often accompany the JAK2^{V617F} allele burden. To study discrete mechanisms associated with MPN development, several mouse models bearing a single JAK2^{V617F} mutation have been generated (reviewed in Dunbar et al[24]). Such models were reported to have either reduced or increased thrombosis, depending on the mouse studied and whether the MPN phenotype is associated with bone

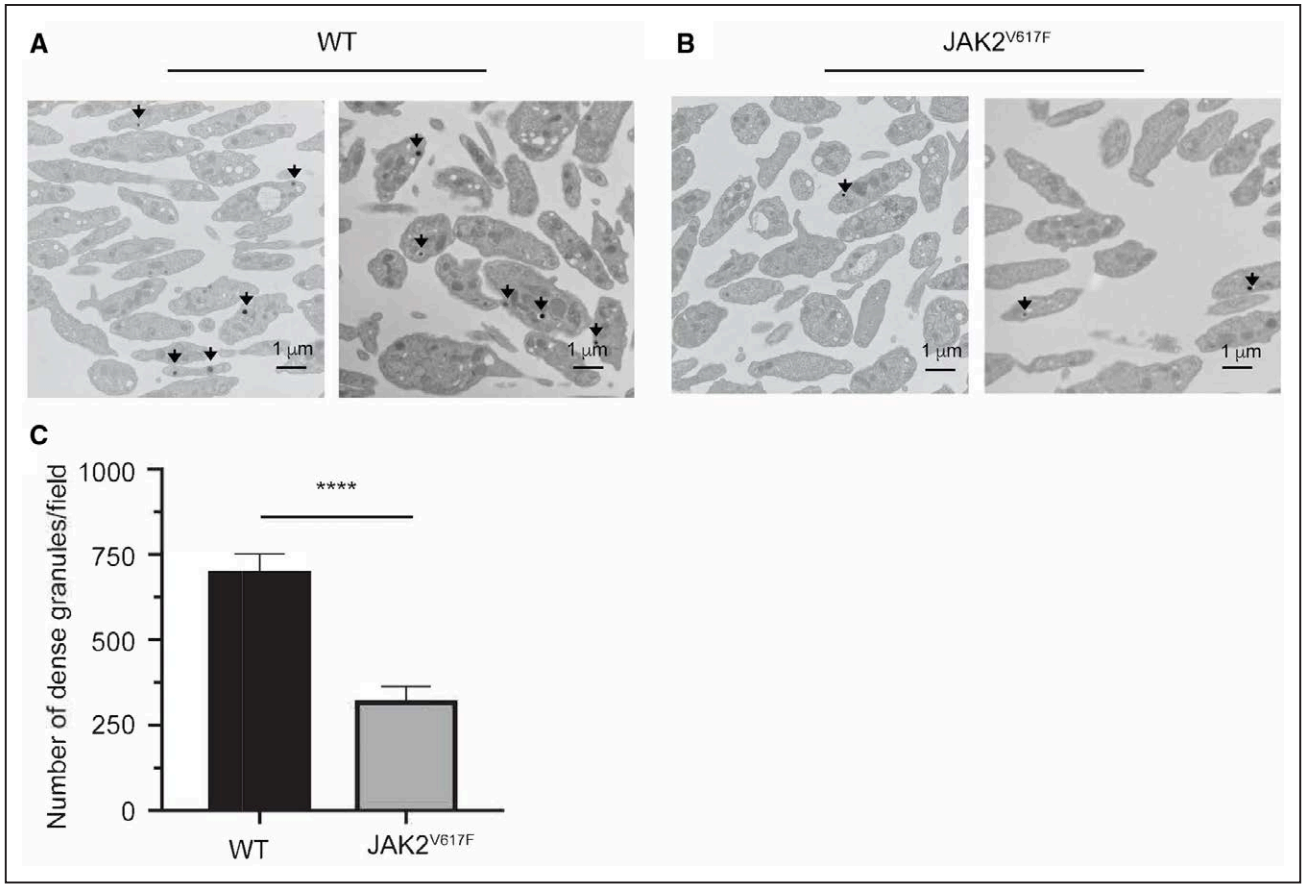

Figure 6. Electron microscopy (EM) reveals a dense granule deficiency in JAK2V617F (janus kinase 2 with valine to phenylalanine substitution on codon 617) mice.

Representative images of EM analysis of platelets derived from 2 wild-type (WT; **A**) or JAK2^{V617F} (**B**) male mice (about 30 wk old). Black arrows represent dense granules found in platelets. **C**, Quantification of dense granules. Shown are averages±SD of 41 fields and 27 fields analyzed for WT and JAK2^{V617F} mice, respectively. Mann Whitney was performed as a 2 tailed test using the Prism software. ****P<0.0001.

marrow fibrosis, or an increased level of specific blood cells. In the current study, we used the Vav1-hJAK2^{V617F} mice (bearing human JAK2^{V617F}), which display hallmarks of PMF, including expansion of the megakaryocyte lineage and a fibrotic bone marrow.[15] The mice have a mild PV phenotype, with increased platelet counts and, anticipated, elevated phosphorylated Stat5 level at baseline (data not shown). This model has allowed us to focus on platelet properties in the context of an isolated, single mutation (JAK2^{V617F}) that was engineered to impact primarily the megakaryocytic lineage and to lead to a fibrotic phenotype. Under these conditions, we made the striking observation that platelets bearing JAK2^{V617F} have reduced aggregation response to collagen, and a significantly reduced number of dense granules, which could explain an observed compromised ability to secret ADP upon platelet activation, and a diminished second wave of activation. The role of JAK2 signaling in controlling platelet dense granule number has never been reported before. Prior studies involving human cohorts identified dense granule storage defects. In one study of 9 patients with myeloproliferative disorders of myelofibrosis, platelets were found to have significant storage pool depletion (measured by ADP/ATP ration and 14C-serotonin platelet disappearance patterns).[25] Another study reported a defect in mepacrine uptake in platelet dense granules in 71% of the PV subjects and in 48% of the ET subjects.[26] Dense granule formation has been reported to be controlled by various factors, such as pallidin transcription.[27] Although there was no significant change in the level of HPS9 between control and JAK2^{V617F} platelets (our unpublished data), future investigations could focus on mechanisms leading to dysregulated dense granule numbers.

P-selectin expression in response to collagen stimulation was decreased in platelets derived from JAK2^{V617F} mice, which could be reflecting the defect in collagen receptor expression and alpha granules. However, further analysis revealed that at baseline there is a tendency for elevated P-selectin expression in JAK2^{V617F} platelets (Figure ID in the Data Supplement). Interestingly, prior studies that looked at α granules in platelets of patients with MPN or myelofibrosis identified a less profound effect in cargo depletion in these granules when compared with dense granules. However, the plasma concentration of platelet factor 4 and β-thromboglobulin

in patients with MPN/myelofibrosis in this study were elevated, when compared with control samples.[25]

In 2 vascular injury models used in our study, thrombus formation was significantly delayed in the Vav1-hJAK2^{V617F} mice. The size of the thrombi in the mutated mice was smaller, compared with controls, suggesting an impact on platelet aggregation properties. At the same time, Vav1-hJAK2^{V617F} mice showed reduced platelet aggregation response to collagen that is associated with diminished levels of platelet cell surface expression of components of the collagen receptors, integrins GPVI and α2. A clear prolonged bleeding time in the PMF mice suggest that this overall PMF phenotype depicts the hemorrhagic events associated with MPN.

The platelet phenotype of the PMF mice we analyzed is reminiscent of a report using the Hasan et al[28] model in which the mouse *Jak2^{V617F}* was knocked-in leading to a clear PV phenotype. In this case too tail bleeding was prolonged, in vitro thrombosis on collagen was reduced in association with diminished levels of the collagen receptor GPVI, and rapidly forming platelet aggregates in a $FeCl_3$-induced thrombosis model were unstable.[6] The mechanism for this observation was not fully explored. Similarly, inducible transgenic expression of human JAK2^{V617F}[29] in hematopoietic and endothelial cells led to thrombocytosis, yet, these mice showed reduced thrombosis following vascular injury associated with compromised von Willebrand factor function.[13] On the contrary, using the ET mouse model generated by Li et al[30] in which human JAK2^{V617F} was knocked-into the genome, the group reported enhanced platelet reactivity and aggregation in vitro and a reduced duration of bleeding in vivo.[7] Moreover, Zhao et al[31] demonstrated that animals that express mouse Jak2^{V617F} at physiological levels, generated by Mullally et al,[32] die of thrombotic events constituting of large vascular occlusions most prominent in lungs and kidneys. Those authors also demonstrated the contribution of Plek2 (pleckstrin-2) in the thrombotic phenotype, which they mostly attributed to elevated red cell mass. Further, a recent study reported that neutrophils from patients with MPN with JAK2^{V617F} mutation tend to form neutrophil extracellular traps and mice with conditional KI of JAK2^{V617F} have an augmented capacity to form neutrophil extracellular traps and increased thrombosis.[14] These opposing results in the different MPN mouse models, albeit induced by JAK2^{V617F}, are likely consistent with the variability of the disorders observed in MPN patients vis-à-vis a balance between augmented incidence of thrombosis versus hemorrhagic events.

Taken together, our study identified a link between JAK2 hyperactivity and a compromised second wave of platelet activation, associated with reduced number of platelet dense granules. Increased tendency for hemorrhages and smaller thrombi in the JAK2^{V617F} mice could at least partially explain the venous thromboembolism and bleeding phenotypes in human PMF.

ARTICLE INFORMATION

Received February 18, 2020; accepted August 4, 2020.

Affiliations

Department of Medicine and Whitaker Cardiovascular Institute (S.M., C.R.T., A.P., O.L., K.R.), Department of Pathology (M.E.B.), Department of Medicine (R.H.B.), and Renal Section, Department of Medicine (V.C.C.), Boston University School of Medicine, MA. Department of Medicine, Brigham and Women's Hospital, Boston MA (A.R., J.I.). Division of Hemostasis and Thrombosis, Department of Medicine, Beth Israel Deaconess Medical Center, Harvard Medical School, Boston, MA (M.Y., G.M.-S., R.F.).

Acknowledgments

K. Ravid, S. Matsuura, and C.R. Thompson generated hypotheses, designed experiments, and analyzed data, and C.R. Thompson and S. Matsuura performed most of the experiments with the help of A. Piasecki. K. Ravid wrote the article with input from C.R. Thompson, S. Matsuura, R.H. Bekendam, and R. Flaumenhaft. O. Leiva, M.E. Belghasem, V.C. Chitalia, G. Merill-Skoloff, M. Yang, and R.H. Bekendam performed and analyzed the in vivo vascular injury models. J. Italiano and A. Ray assisted in electron microscopy studies.

Sources of Funding

This work was supported by National Heart, Lung, and Blood Institute (NIHLBI) grant R01HL136363 to K. Ravid and grant R35HL135775 to R. Flaumenhaft. K. Ravid is an established investigator with the American Heart Association. C.R. Thompson was supported by NHLBI Cardiovascular Research Training grant T32 HL007224, and M. Yang is supported by T32HL007917. S. Matsuura was supported by the National Institutes of Health ORIP SERCA K01 award 1K01_D025290-01A1.

Disclosures

None.

REFERENCES

1. Vainchenker W, Kralovics R. Genetic basis and molecular pathophysiology of classical myeloproliferative neoplasms. *Blood.* 2017;129:667–679. doi: 10.1182/blood-2016-10-695940
2. Tefferi A. Primary myelofibrosis: 2017 update on diagnosis, risk-stratification, and management. *Am J Hematol.* 2016;91:1262–1271. doi: 10.1002/ajh.24592
3. Arber DA, Orazi A, Hasserjian R, Thiele J, Borowitz MJ, Le Beau MM, Bloomfield CD, Cazzola M, Vardiman JW. The 2016 revision to the world health organization classification of myeloid neoplasms and acute leukemia. *Blood.* 2016;127:2391–2405. doi: 10.1182/blood-2016-03-643544
4. Li J, Kent DG, Chen E, Green AR. Mouse models of myeloproliferative neoplasms: JAK of all grades. *Dis Model Mech.* 2011;4:311–317. doi: 10.1242/dmm.006817
5. Tefferi A. Myeloproliferative neoplasms: a decade of discoveries and treatment advances. *Am J Hematol.* 2016;91:50–58. doi: 10.1002/ajh.24221
6. Lamrani L, Lacout C, Ollivier V, Denis CV, Gardiner E, Ho Tin Noe B, Vainchenker W, Villeval JL, Jandrot-Perrus M. Hemostatic disorders in a JAK2V617F-driven mouse model of myeloproliferative neoplasm. *Blood.* 2014;124:1136–1145. doi: 10.1182/blood-2013-10-530832
7. Hobbs CM, Manning H, Bennett C, Vasquez L, Severin S, Brain L, Mazharian A, Guerrero JA, Li J, Soranzo N, et al. JAK2V617F leads to intrinsic changes in platelet formation and reactivity in a knock-in mouse model of essential thrombocythemia. *Blood.* 2013;122:3787–3797. doi: 10.1182/blood-2013-06-501452
8. Barbui T, Carobbio A, Cervantes F, Vannucchi AM, Guglielmelli P, Antonioli E, Alvarez-Larrán A, Rambaldi A, Finazzi G, Barosi G. Thrombosis in primary myelofibrosis: incidence and risk factors. *Blood.* 2010;115:778–782. doi: 10.1182/blood-2009-08-238956
9. Rungjirajittranon T, Owattanapanich W, Ungprasert P, Siritanaratkul N, Ruchutrakool T. A systematic review and meta-analysis of the prevalence of thrombosis and bleeding at diagnosis of Philadelphia-negative myelopro-

liferative neoplasms. *BMC Cancer.* 2019;19:184. doi: 10.1186/s12885-019-5387-9
10. Rupoli S, Goteri G, Picardi P, Micucci G, Canafoglia L, Scortechini AR, Federici I, Giantomassi F, Da Lio L, Zizzi A, et al. Thrombosis in essential thrombocytemia and early/prefibrotic primary myelofibrosis: the role of the WHO histological diagnosis. *Diagn Pathol.* 2015;10:29. doi: 10.1186/s13000-015-0269-1
11. Landolfi R. Bleeding and thrombosis in myeloproliferative disorders. *Curr Opin Hematol.* 1998;5:327–331. doi: 10.1097/00062752-199809000-00004
12. Li J, Kent DG, Godfrey AL, Manning H, Nangalia J, Aziz A, Chen E, Saeb-Parsy K, Fink J, Sneade R, et al. JAK2V617F homozygosity drives a phenotypic switch in myeloproliferative neoplasms, but is insufficient to sustain disease. *Blood.* 2014;123:3139–3151. doi: 10.1182/blood-2013-06-510222
13. Etheridge SL, Roh ME, Cosgrove ME, Sangkhae V, Fox NE, Chen J, López JA, Kaushansky K, Hitchcock IS. JAK2V617F-positive endothelial cells contribute to clotting abnormalities in myeloproliferative neoplasms. *Proc Natl Acad Sci U S A.* 2014;111:2295–2300. doi: 10.1073/pnas.1312148111
14. Wolach O, Sellar RS, Martinod K, Cherpokova D, McConkey M, Chappell RJ, Silver AJ, Adams D, Castellano CA, Schneider RK, et al. Increased neutrophil extracellular trap formation promotes thrombosis in myeloproliferative neoplasms. *Sci Transl Med.* 2018;10:eaan8292. doi: 10.1126/scitranslmed.aan8292
15. Xing S, Wanting TH, Zhao W, Ma J, Wang S, Xu X, Li Q, Fu X, Xu M, Zhao ZJ. Transgenic expression of JAK2V617F causes myeloproliferative disorders in mice. *Blood.* 2008;111:5109–5117. doi: 10.1182/blood-2007-05-091579
16. Leiva O, Ng SK, Matsuura S, Chitalia V, Lucero H, Findlay A, Turner C, Jarolimek W, Ravid K. Novel lysyl oxidase inhibitors attenuate hallmarks of primary myelofibrosis in mice. *Int J Hematol.* 2019;110:699–708. doi: 10.1007/s12185-019-02751-6
17. Matsuura S, Mi R, Koupenova M, Eliades A, Patterson S, Toselli P, Thon J, Italiano JE Jr, Trackman PC, Papadantonakis N, et al. Lysyl oxidase is associated with increased thrombosis and platelet reactivity. *Blood.* 2016;127:1493–1501. doi: 10.1182/blood-2015-02-629667
18. Flaumenhaft R, Dilks JR, Rozenvayn N, Monahan-Earley RA, Feng D, Dvorak AM. The actin cytoskeleton differentially regulates platelet alpha-granule and dense-granule secretion. *Blood.* 2005;105:3879–3887. doi: 10.1182/blood-2004-04-1392
19. Liu Y, Jennings NL, Dart AM, Du XJ. Standardizing a simpler, more sensitive and accurate tail bleeding assay in mice. *World J Exp Med.* 2012;2:30–36. doi: 10.5493/wjem.v2.i2.30
20. Higgins SJ, De Ceunynck K, Kellum JA, Chen X, Gu X, Chaudhry SA, Schulman S, Libermann TA, Lu S, Shapiro NI, et al. Tie2 protects the vasculature against thrombus formation in systemic inflammation. *J Clin Invest.* 2018;128:1471–1484. doi: 10.1172/JCI97488
21. Hultcrantz M, Björkholm M, Dickman PW, Landgren O, Derolf ÅR, Kristinsson SY, Andersson TML. Risk for arterial and venous thrombosis in patients with myeloproliferative neoplasms: a population-based cohort study. *Ann Intern Med.* 2018;168:317–325. doi: 10.7326/M17-0028
22. Bertozzi I, Bogoni G, Biagetti G, Duner E, Lombardi AM, Fabris F, Randi ML. Thromboses and hemorrhages are common in MPN patients with high JAK2V617F allele burden. *Ann Hematol.* 2017;96:1297–1302. doi: 10.1007/s00277-017-3040-8
23. Ball S, Thein KZ, Maiti A, Nugent K. Thrombosis in Philadelphia negative classical myeloproliferative neoplasms: a narrative review on epidemiology, risk assessment, and pathophysiologic mechanisms. *J Thromb Thrombolysis.* 2018;45:516–528. doi: 10.1007/s11239-018-1623-4
24. Dunbar A, Nazir A, Levine R. Overview of transgenic mouse models of myeloproliferative neoplasms (MPNs). *Curr Protoc Pharmacol.* 2017;77:14.40.1–14.40.19. doi: 10.1002/cpph.23
25. Malpass TW, Savage B, Hanson SR, Slichter SJ, Harker LA. Correlation between prolonged bleeding time and depletion of platelet dense granule ADP in patients with myelodysplastic and myeloproliferative disorders. *J Lab Clin Med.* 1984;103:894–904.
26. Coucelo M, Caetano G, Sevivas T, Almeida Santos S, Fidalgo T, Bento C, Fortuna M, Duarte M, Menezes C, Ribeiro ML. JAK2V617F allele burden is associated with thrombotic mechanisms activation in polycythemia vera and essential thrombocythemia patients. *Int J Hematol.* 2014;99:32–40. doi: 10.1007/s12185-013-1475-9
27. Mao GF, Goldfinger LE, Fan DC, Lambert MP, Jalagadugula G, Freishtat R, Rao AK. Dysregulation of PLDN (pallidin) is a mechanism for platelet dense granule deficiency in RUNX1 haplodeficiency. *J Thromb Haemost.* 2017;15:792–801. doi: 10.1111/jth.13619
28. Hasan S, Lacout C, Marty C, Cuingnet M, Solary E, Vainchenker W, Villeval JL. JAK2V617F expression in mice amplifies early hematopoietic cells and gives them a competitive advantage that is hampered by IFNα. *Blood.* 2013;122:1464–1477. doi: 10.1182/blood-2013-04-498956
29. Tiedt R, Hao-Shen H, Sobas MA, Looser R, Dirnhofer S, Schwaller J, Skoda RC. Ratio of mutant JAK2-V617F to wild-type Jak2 determines the MPD phenotypes in transgenic mice. *Blood.* 2008;111:3931–3940. doi: 10.1182/blood-2007-08-107748
30. Li J, Spensberger D, Ahn JS, Anand S, Beer PA, Ghevaert C, Chen E, Forrai A, Scott LM, Ferreira R, et al. JAK2 V617F impairs hematopoietic stem cell function in a conditional knock-in mouse model of JAK2 V617F-positive essential thrombocythemia. *Blood.* 2010;116:1528–1538. doi: 10.1182/blood-2009-12-259747
31. Zhao B, Mei Y, Cao L, Zhang J, Sumagin R, Yang J, Gao J, Schipma MJ, Wang Y, Thorsheim C, et al. Loss of pleckstrin-2 reverts lethality and vascular occlusions in JAK2V617F-positive myeloproliferative neoplasms. *J Clin Invest.* 2018;128:125–140. doi: 10.1172/JCI94518
32. Mullally A, Lane SW, Ball B, Megerdichian C, Okabe R, Al-Shahrour F, Paktinat M, Haydu JE, Housman E, Lord AM, et al. Physiological Jak2V617F expression causes a lethal myeloproliferative neoplasm with differential effects on hematopoietic stem and progenitor cells. *Cancer Cell.* 2010;17:584–596. doi: 10.1016/j.ccr.2010.05.015